

Potassium Ion Accumulation in a Periaxonal Space and Its Effect on the Measurement of Membrane Potassium Ion Conductance

William J. Adelman, Jr., Yoram Palti* and Joseph P. Senft**

Laboratory of Biophysics, IR, National Institute of Neurological Diseases and Stroke,
National Institutes of Health, Bethesda, Md. 20014 and
The Marine Biological Laboratory, Woods Hole, Mass. 02543

Received 9 April 1973

Summary. Potassium currents of various durations were obtained from squid giant axons voltage-clamped in artificial seawater solutions containing sufficient tetrodotoxin to block the sodium conductance completely. From instantaneous potassium current-voltage relations, the reversal potentials immediately at the end of these currents were determined. On the basis of these reversal potential measurements, the potassium ion concentration gradient across the membrane was shown to decrease as the potassium current duration increased. The kinetics of this change was shown to vary monotonically with the potassium ion efflux across the membrane estimated from the integral over time of the potassium current divided by the Faraday, and to be independent of both the external sodium ion concentration and the presence or absence of membrane series resistance compensation. It was assumed that during outward potassium current flow, potassium ions accumulated in a periaxonal space bounded by the membrane and an external diffusion barrier. A model system was used to describe this accumulation as a continuous function of the membrane currents. On this basis, the mean periaxonal space thickness and the permeability of the external barrier to K^+ were found to be 357 Å and 3.21×10^{-4} cm/sec, respectively. In hyperosmotic seawater, the value of the space thickness increased significantly even though the potassium currents were not changed significantly. Values of the resistance in series with the membrane were calculated from the values of the permeability of the external barrier and these values were shown to be roughly equivalent to series resistance values determined by current clamp measurements. Membrane potassium ion conductances were determined as a function of time and voltage. When these were determined from data corrected for the potassium current reversal potential changes, larger maximal potassium conductances were obtained than were obtained using a constant reversal potential. In addition, the potassium conductance turn-on with time at a variety of membrane potentials was shown to be slower when potassium conductance values were obtained using a variable reversal potential than when using a constant reversal potential.

* *Present address:* Department of Physiology and Biophysics, The Technion Medical School, Haifa, Israel.

** *Present address:* Department of Biology, Juniata College, Huntingdon, Pa. 16652.

The squid giant axon is enclosed by an external sheath composed of two layers, an outer layer of connective tissue cells and collagen fibers and an inner layer of Schwann cells (Geren & Schmitt, 1953, 1954; Villegas & Villegas, 1960; Baker, Hodgkin & Shaw, 1962; Villegas, 1969). These two layers are separated by a basement membrane (Geren & Schmitt, 1954), composed of a ground substance and ultra-fine collagen fibers (J. Metuzals, *personal communication*; also see Metuzals & Izzard, 1969, Fig. 20). A periaxonal space or cleft having a radial dimension of about 100 Å is found between the axolemma and the inner boundary of the Schwann cells (Geren & Schmitt, 1953, 1954). The Schwann cells are separated from each other by 60- to 100 Å-thick clefts or channels which extend continuously from the periaxonal space to the basement membrane (Frankenhaeuser & Hodgkin, 1956; Villegas & Villegas, 1960). Villegas, Caputo and Villegas (1962) have shown that water diffuses freely through the clefts but is limited mainly by the long path length and relatively small cross-sectional areas.

During a single impulse, the extra potassium ion efflux above the resting efflux through 1 cm² of membrane has been estimated to be about 4×10^{-12} M in squid axons (Keynes, 1951; Keynes & Lewis, 1951; Shanes, 1954). This extra potassium ion efflux does not instantaneously diffuse away from the immediate external surface of the axolemma of the giant axon. Using the membrane potential during the undershoot phase of the action potential to estimate the potassium ion gradient across the squid axon membrane, Frankenhaeuser and Hodgkin (1956) have shown increases in potassium concentration in an assumed periaxonal space during repetitive firing. After a single impulse, the apparent potassium concentration $[K]_s$ was found to increase by 1 to 2 mM above the concentration of the external bulk solution K_o (normally $K_o = 10$ mM). At firing rates of about 100/sec, the concentration in the space approached 30 mM. These changes were attributed to differences between potassium fluxes across the axolemma and across the external sheath, i.e., the Schwann cell-connective tissue layers. Frankenhaeuser and Hodgkin (1956) showed that membrane potassium currents during voltage clamp pulses also produce changes in $[K]_s$ that are related to the integral of the current with respect to time and that these $[K]_s$ changes can be accounted for by a potassium accumulation model derived from the action potential studies.

Changes in surface ion concentration with activity or passage of electric currents are not limited to squid axons. Orkand, Nicholls and Kuffler (1966), Baylor and Nicholls (1969*a*), and others (*cf.* Adelman & Palti, 1972*a*) have marshalled an array of evidence which indicates that during repetitive firing the concentration of potassium ions changes at the external surface of

several neurons. A similar phenomenon was described in *Chara* cells by Barry and Hope (1969*a, b*). From the above findings, it is apparent that under a variety of conditions one cannot assume that E_K remains constant during nervous activity or under voltage clamp conditions.

In the work reported here, voltage clamp experiments were performed and a multicompartamental model was applied to the results of these experiments to investigate the apparent potassium ion concentration changes, $\delta[K]_s$, in the aqueous medium immediately adjacent to the axon membrane. The model was derived from Frankenhaeuser and Hodgkin's hypothesis 1 (1956, p. 366) which assumed that potassium ion accumulation occurred in the periaxonal space because of an imbalance between membrane and external barrier ionic fluxes. The early part of this work was patterned after the voltage clamp experiments analyzed by Frankenhaeuser and Hodgkin (1956), with an initial object of testing the potassium accumulation hypothesis in *Loligo pealei* axons. The $[K]_s$ changes were calculated on the basis of the changes in the apparent reversal potential E_K of the potassium current. The values of E_K were determined from the measured values of E_M corresponding to the zero crossover points of the curves relating the values of the instantaneous potassium current to E_M . A variety of tests of the analytical methods and of the multicompartamental model were carried out.

Inasmuch as $[K]_s$ varies as a function of outward potassium current flow across the membrane, the driving force of this current ($E - E_K$) is also a variable. This work will show that it is possible to obtain a proper set of $g_K(t, E_M)$ values once the values of E_K are determined as a function of $I_K(t, E_M)$. Thus, membrane conductance parameter values can be obtained that are uncontaminated by periaxonal potassium accumulation. These values should represent the membrane behavior more accurately.

Materials and Methods

Single giant axons were prepared from the hindmost stellar nerve of the squid, *Loligo pealei*. These axons were carefully cleaned of all surrounding small nerve fibers and any loose connective tissue. The axons were then mounted in a horizontal voltage clamp chamber. External solutions were: artificial seawater (ASW), ASW having a tetrodotoxin concentration of 100 nM (TTX ASW), 100 nM TTX ASW made 10% hyperosmotic by the addition of NaCl, and ASW in which the NaCl was replaced with Tris Cl. Table 1 lists the composition of these solutions.

Axons were voltage-clamped by a modification of the Cole and Moore (1960) method. This modification was described by Adelman and Palti (1969*a*). Membrane currents I_M in the voltage clamp were measured as a function of time when the membrane potential E_M was stepped from one value to another. Membrane potentials were measured between an internal microelectrode (1 to 3 M Ω), whose tip was just inside the

Table 1. Composition of solutions

Solution	[Na ⁺] (mM)	[K ⁺] (mM)	[Tris ⁺] (mM)	[Mg ⁺⁺] (mM)	[Ca ⁺⁺] (mM)	[Cl ⁻] (mM)	[TTX] (nM)	pH at 5 °C
ASW	440	10	10	50	10	580	0	7.4
TTX-ASW	440	10	10	50	10	580	100	7.4
Tris-ASW	0	10	450	50	10	580	0	7.4
10% Hyper- osmotic ASW	547	10	10	50	10	687	100	7.4
Low Na ASW	240	10	210	50	10	580	0	7.4
Low Na ASW	0	25	425	50	10	570	0	7.4
Low Na ASW	25	25	400	50	10	570	0	7.4
Low Na ASW	50	25	375	50	10	570	0	7.4
Low Na ASW	100	25	325	50	10	570	0	7.4
Low Na ASW	200	25	225	50	10	570	0	7.4
Low Na ASW	400	25	25	50	10	570	0	7.4

plasmalemma and an external microelectrode ($<0.5 \text{ M}\Omega$) located with its tip just outside the Schwann cell-connective tissue layer. Both microelectrodes were filled with 3 M KCl. These were connected to a balanced pair of Calomel half-cells. The internal electrode was compensated for tip capacity by feedback from an impedance converter pre-amplifier. No corrections were made for electrode junction potentials. Before penetration of the axon with the internal microelectrode, any potential difference between the two electrodes was nulled with the two tips in ASW. In a number of the experiments, the resistance in series with the membrane R_s (Hodgkin, Huxley & Katz, 1952) was compensated by feedback (Moore & Cole, 1963). The method for determining R_s involved measuring in current clamp the voltage response to a current pulse flowing between the axial wire electrode and the external platinum black cell electrodes. Voltage was recorded directly from the axial wire and current was measured at the central external metal electrode through an operational amplifier. The upper frequency response for these measurements was on the order of 1 MHz. These current clamp measurements were made twice before each voltage clamp experiment: first, with the axial wire in the cell without the axon, and second, with axial wire within the axon to be subsequently voltage-clamped. From the first measurement the resistance of the metal electrodes and the seawater between the electrodes was determined. From the second measurement, the resistance of the electrodes, axoplasm, Schwann cell-connective tissue layer and seawater was determined. For overly damped current pulses with a rise time of about 1 μsec or less, a seawater specific resistance of 25 Ωcm , and an axoplasm specific resistance of 37 Ωcm (David O. Carpenter, *personal communication*; Carpenter, Hovey & Bak, 1971, 1972), the resistance of the Schwann cell layer, i.e., the resistance in series with the membrane of the axon between the internal and external microelectrodes, was found to be 0.77 ± 0.31 (SD) Ωcm^2 . Since sufficient resolution, using a voltage deflection of one mV/cm and a sweep speed of one $\mu\text{sec/cm}$, could be obtained on the polaroid pictures of the oscilloscope traces, these measurements and the subsequent calculations could be made within a few minutes. A full description of the method, the derivation of the equations used in the calculations, and R_s results obtained on both *Loligo* and *Myxicola* axons is in preparation (Binstock, Adelman, Senft & Lecar).

Results

The Instantaneous Potassium Current-Voltage Relation

The initial object of this work was to quantify the relation between the efflux of potassium ions carried through the potassium conductance during a voltage clamp and the extent of potassium ion accumulation in the periaxonal space. Frankenhaeuser and Hodgkin (1956, p. 361) have shown that for potassium currents of various durations the reversal potential immediately at the end of each of these currents can be obtained from the current "tails" (Hodgkin & Huxley, 1952*a*) following these currents. Hodgkin and Huxley (1952*a*) showed that, upon stepping the membrane potential from a depolarized value to a more hyperpolarized value, the membrane current would instantaneously change to a new value which then declined exponentially with time. This declining current was called the "tail" current. To make use of this method, initially E_M was clamped to a holding value E_0 equal to the resting membrane potential. During a typical experiment, E_M was stepped from E_0 to a depolarized pre-pulse value E_1 for a duration t_1 . Then, E_M was stepped to a new value E_2 for a few msec before returning to E_0 . This sequence of pulses was repeated several times at a frequency of 0.2/sec, keeping E_1 and t_1 constant and varying E_2 . The value of t_1 was then changed and the process was repeated for the same E_1 and another set of E_2 values.

On the basis of membrane currents in response to hyperpolarizing pulses, the transient capacity current initiated upon stepping E_M from E_1 to E_2 was shown to peak and decline almost completely within 15 μ sec after the onset of E_2 . However, a very small fraction of the capacity current persists for about 50 μ sec after the step in potential (*cf.* Hodgkin *et al.*, 1952, Fig. 16). Therefore, the amplitude of the ionic current, immediately after the step from E_1 to E_2 was obtained by extrapolating the exponential portion (from 0.1 to 1 msec after the step) of each tail current back through the capacity transient to the onset of E_2 . We shall refer to the initial value of I_{tail} as I_{tail}^0 .

Fig. 1 illustrates typical records of membrane currents and potentials recorded from a voltage-clamped giant axon externally perfused with 100 nM tetrodotoxin ASW. Each record contains two (doubly exposed) upper and lower oscilloscope traces. The upper traces represent the recorded membrane potential and the lower traces the recorded membrane currents. As can be seen in the upper traces, pulse 1 is always to a membrane potential (E_1) of zero mV; pulse 2 is either to a membrane potential (E_2) of -36 mV or -76 mV. By examining the lower traces, it can be seen that, as the duration of pulse 1 increases, the outward current increases, reaches a

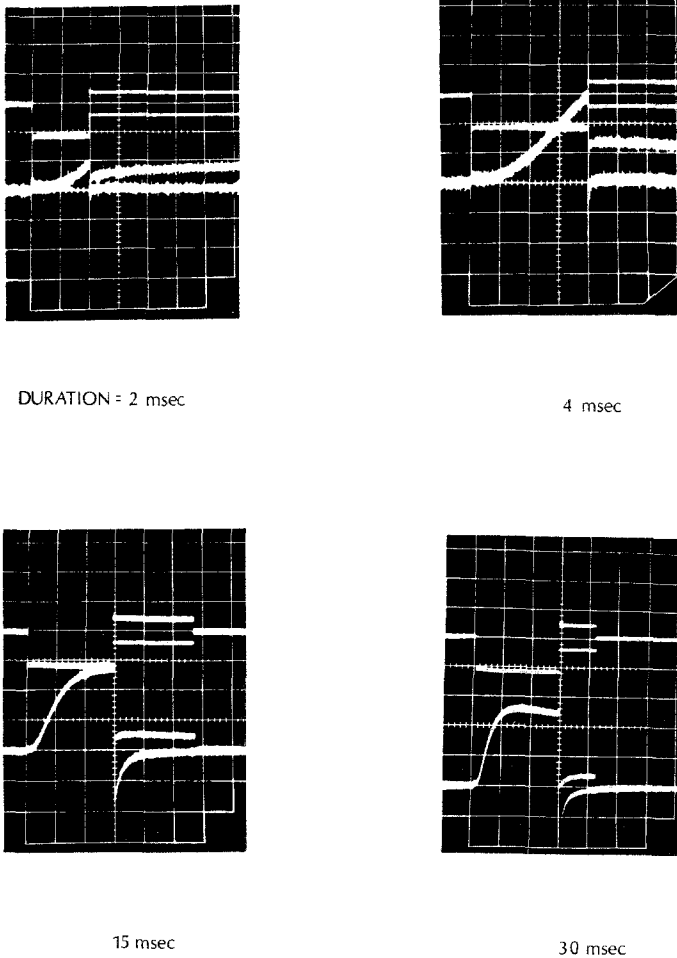


Fig. 1. Records of membrane potentials and currents recorded from a voltage-clamped squid giant axon bathed in 100 nM TTX ASW. Ordinates in all four frames for upper traces: membrane potential, 50 mV/major division; ordinates for lower traces: membrane current, $0.5 \text{ mamp} \cdot \text{cm}^{-2}$ /major division for two upper frames and $1 \text{ mamp} \cdot \text{cm}^{-2}$ /major division for two lower frames. Abscissas in two upper frames: 1 msec/major division, in lower left frame: 5 msec/major division, and in lower right frame: 10 msec/major division. The currents were elicited by stepping the membrane potential E_M from the holding potential value of -56 mV to a value of E_1 of 0 mV and then at an interval of t_1 to $E_2 = -36 \text{ mV}$, or $E_2 = -76 \text{ mV}$. Values of t_1 are given below each of the four recordings. The lower traces show the instantaneous changes in I_K elicited by stepping E_M from the value of E_1 to E_2 and the shapes of the tail currents which follow. Axon 4. A series resistance of $1 \Omega \text{cm}^2$ was compensated by positive feedback and this is indicated in the membrane potential records. Temperature 6°C

maximum at 17 msec, and then declines or "droops" as the pulse duration increases to 30 msec. These outward currents in response to pulse 1 are

followed by two "tail" currents in response to the two amplitudes of pulse 2. In each recording of the membrane current, the lower tail current was recorded for $E_2 = -76$ mV. It is apparent that as t_1 increases, these particular tail currents have larger initial inward values (I_{tail}^0 values).

Inasmuch as TTX dose-response studies on squid axons (Cuervo & Adelman, 1970) have shown that 100 nM TTX completely blocks the sodium conductance, we shall assume that the potassium current is the membrane current recorded in 100 nM TTX ASW minus the leakage current component. The potassium current may be described by the expression (Hodgkin & Huxley, 1952*b*):

$$I_K = \bar{g}_K n^4 (E - E_K) \quad (1)$$

where \bar{g}_K is the maximal potassium conductance (about 40 mmho) and n is the Hodgkin-Huxley (1952*b*) potassium conductance parameter. When I_{tail}^0 is determined, $E_M = E_2$. However, since n changes relatively slowly (its time

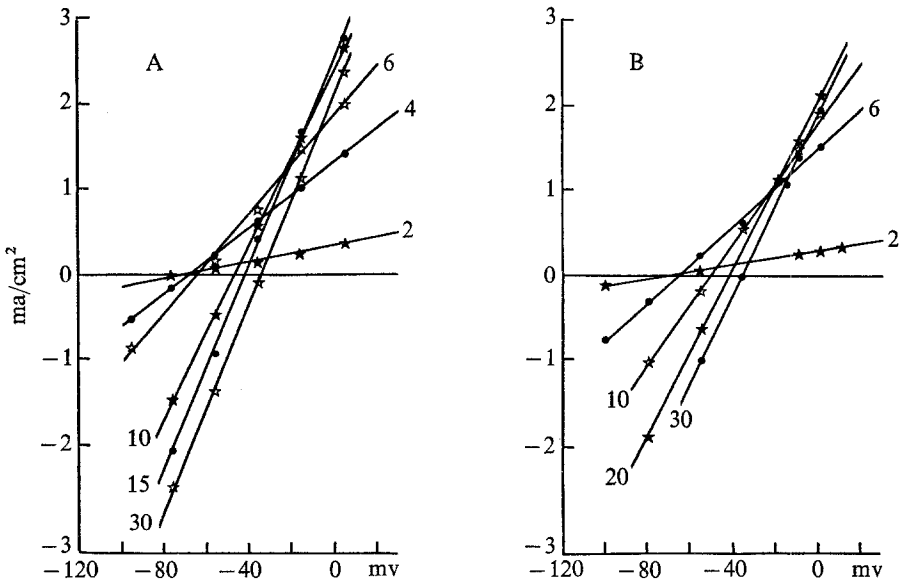


Fig. 2. Instantaneous membrane current-potential relations as a function of pulse duration t_1 . *A*: series resistance of $1.0 \Omega\text{cm}^2$ compensated by feedback. *B*: no series resistance compensation. Initial values of tail currents were recorded from a voltage-clamped squid axon at the end of a depolarizing pulse E_1 when the membrane potential was stepped to a variety of post-pulse potentials E_2 . The points correspond to the values of the potassium current tails at the beginning of E_2 , corrected for leakage and capacity currents. E_1 in all cases was 0 mV. The values of E_2 are given on the abscissa. Axon 4, bathed in 100 nM TTX ASW. Temperature was $6.0 \pm 0.1^\circ\text{C}$. Each set of points corresponds to a given duration t_1 of E_1 . Values of t_1 are given adjacent to each set of current values. Note the effect of the duration of the depolarizing pulse on the potassium reversal potential as indicated by the zero current crossover values

constant varies from 1 to 10 msec), the value of n at the onset of E_2 is still that determined previously by E_1 and t_1 at the time the initial value of the tail current I_{tail}^0 is measured. Therefore, regardless of the value of E_2 , the value of n at the onset of E_2 is the same for any specific E_1 and pre-pulse duration t_1 . Since \bar{g}_K and n have finite values for $n > 0$, following Eq. (1), I_{tail}^0 equals zero only when $E_2 - E_K = 0$, i.e., when $E_2 = E_K$. Experimental values of I_{tail}^0 corrected for leakage and capacity currents were plotted against E_2 for each t_1 value. Fig. 2 is illustrative of these plots. The assumption that for any specific E_1 and t_1 , \bar{g}_K and n^4 are constant for a set of I_{tail}^0 values implies that, for any specific t_1 and E_1 , the instantaneous I_{tail}^0 vs. E_2 relation should be linear Eq. (1).

Notice the straightness of the lines fitting the points shown in Fig. 2. Later we will use the slopes of these instantaneous current-voltage relations to determine the membrane potassium conductance g_K for E_1, t_1 .

Relation between the Potassium Current Reversal Potential and the Membrane Potassium Ion Efflux

From the zero current points in Fig. 2A and B, E_K values were obtained. Fig. 3 relates these to values of the potassium ion flux over the interval from $t=0$ to $t=t_1$, $M_K(t_1)$, through the axolemma of a typical axon. The flux was obtained from the following relation (Frankenhaeuser & Hodgkin, 1956):

$$M_K(t_1) = \frac{1}{F} \int_0^{t_1} (I_K) dt \quad (2)$$

where F is the Faraday, 96,500 amp sec/mole. As all $I_K(t_1)$ values were outward, $M_K(t_1)$ can be taken as the net potassium efflux over the interval from $t=0$ to $t=t_1$ in M/cm². Note that the kinetics of the E_K change are related to the $\int_0^{t_1} (I_K) dt$ and are only a function of R_s compensation in that somewhat larger currents (and hence effluxes) are obtained with R_s compensation than without.

One possibility is that these E_K changes arise from a shift in the potassium current reversal potential resulting from contributions of other charge carriers than K^+ to the delayed current¹. One likely alternate charge carrier is sodium. A number of experiments excluded this possibility. Fig. 4 shows that the change in E_K as a function of $\frac{1}{F} \int_0^{t_1} (I_K) dt$ is not influenced by the

¹ We shall call the delayed current I_K inasmuch as K^+ is the predominant charge carrier for this current.

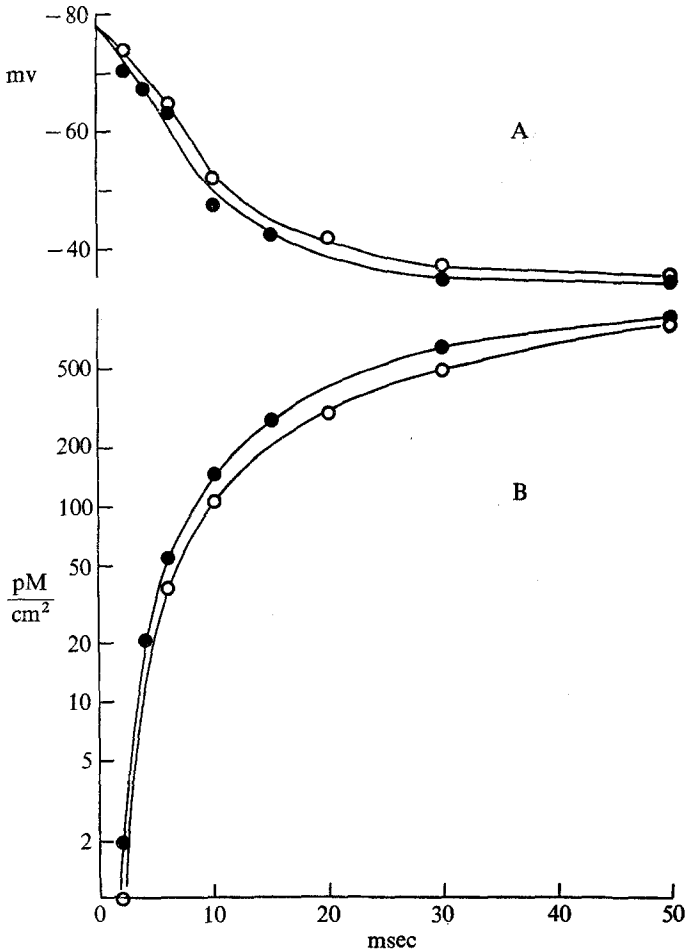


Fig. 3. Correlation between potassium current reversal potential values (*A*, ordinate) at time t_1 (abscissa) with potassium ion efflux values $M_K(t_1)$, (*B*, ordinate), obtained from the definite integral over time (from 0 to t_1 msec) of the potassium current divided by the Faraday both plotted as a function of the duration t_1 (abscissa in *B*) of a membrane depolarization from -56 to 0 mV. E_K values in *A* were determined from the zero current crossover points of current potential relations shown in Fig. 2*A* (filled circles) and in Fig. 2*B* (open circles). Filled circles: R_s of $1 \Omega\text{cm}^2$ compensated by feedback; open circles: R_s uncompensated. Axon 4. Temperature 6°C

external sodium ion concentration $[\text{Na}]_0$. E_K vs. t curves obtained from two axons, selected for having similar $\int_0^{t_1} (I_K) dt$ vs. t_1 curves, are compared. One axon was externally perfused with TTX ASW in which $[\text{Na}]_0 = 440$ mM, and the other axon was externally perfused with ASW in which all the NaCl was replaced with Tris Cl. Values of E_K were only measured from $t_1 = 4$ msec

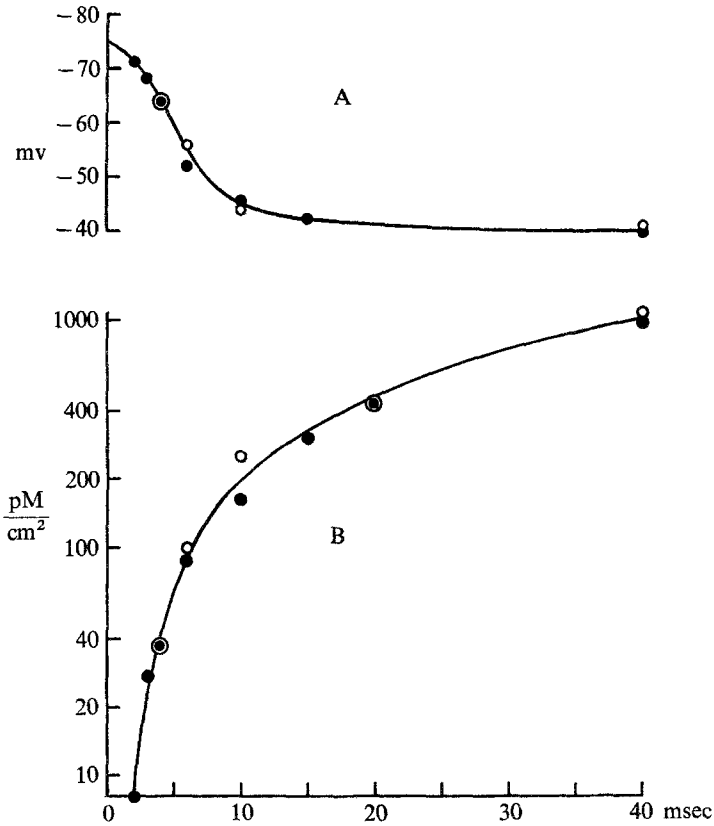


Fig. 4. Correlation between the potassium current reversal potential (*A*, ordinate) at time t_1 and the potassium ion efflux $M_K(t_1)$, (*B*, ordinate), both plotted against the duration (*B*, abscissa) of a membrane depolarization. See legend of Fig. 3 for further details. Filled circles: axon 7 bathed in 100 nM TTX-ASW; open circles: axon 8 bathed in Na-free ASW. See text

to 40 msec in the axon externally perfused with Tris⁺ ASW so as to avoid the transient sodium conductance which at $E_1 = 0$ mV had a duration of about 4 msec. Other experiments in which $[Na]_0$ was varied between zero and 440 mM indicated that I_K was not a function of Na_0 .

Two typical experiments are illustrated in Fig. 5. In *A*, the value of I_K at $t_1 = 14$ msec is shown as a function of E_1 for external perfusion with ASW containing 440 mM Na and with ASW containing 240 mM Na. No significant difference in the I_K vs. E_M relation is seen for a sodium concentration change of 200 mM. In *B*, the value of I_K at $t_1 = 30$ msec is shown as a function of E_1 for external perfusion with a variety of $[Na]_0$. In *B*, $[K]_0$ was 25 mM to show that even at a raised external potassium ion concentration, the effect of Na ions on I_K is nil. While no specific experiments were

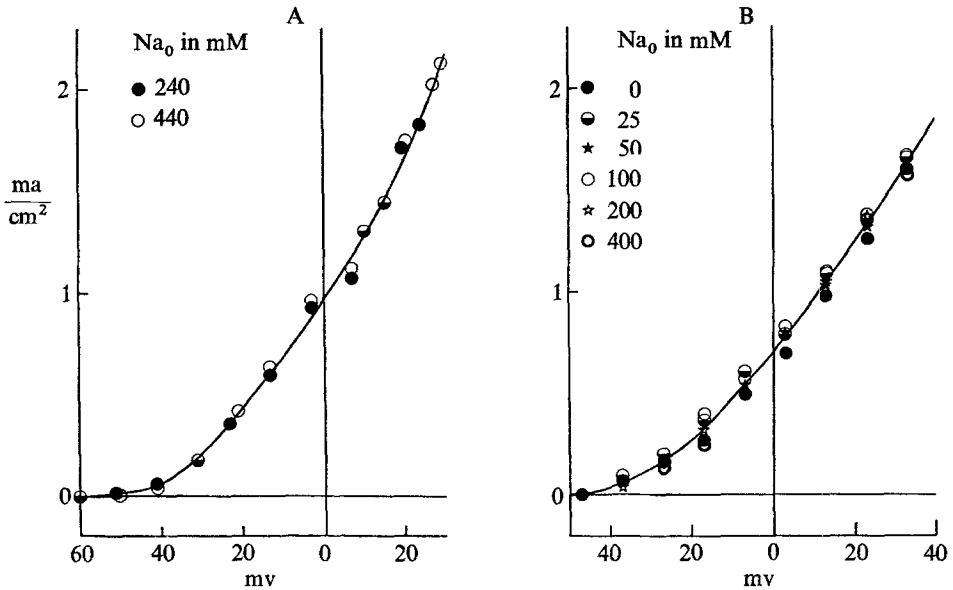


Fig. 5. Steady-state potassium current-voltage relations as a function of the external sodium concentration Na_0 . Values of Na_0 are on the figure. *A*: axon 9 with $K_0 = 10$ mM. *B*: axon 10 with $K_0 = 25$ mM. See text for further details

run to exclude anion contributions, previous experience suggested that anions do not contribute as charge carriers to I_K .

Prediction of $[K]_s$ Changes from a Multicompartmental Model

Frankenhaeuser and Hodgkin (1956) proposed a model for predicting changes in periaxonal potassium ion concentration as a function of membrane current during a membrane voltage clamp. This model (hypothesis 1) assumed that diffusion of potassium ions away from the axolemma can be described as if it were restricted by a thin outer barrier separated from the axolemma by an aqueous space several hundred Å thick. Diffusion in the space was assumed to be rapid and to result in a constant concentration throughout the space at any instant in time. This phenomenological space may be identified with the periaxonal space (Geren & Schmitt, 1953, 1954) and a small fraction of the Schwann cell clefts (Villegas & Villegas, 1960), while the barrier may be the Schwann cells and the connective tissues (Villegas *et al.*, 1962).

In such a multicompartmental (axoplasm, periaxonal space, Schwann cell clefts, and external solution) model, potassium ion concentration in the phenomenological periaxonal aqueous space, $[K]_s$, depends on the initial

potassium concentration and the potassium ion fluxes into and out of the space.

The increment in potassium concentration in M/cm^3 in the space, $\delta[\text{K}]_s$, as a result of a potassium flux in $\text{M}/\text{cm}^2 \times \text{sec}$ into the space, M_K , during the interval from 0 to t_1 can be described by the following equation (cf. Adelman & Palti, 1969*b*, 1972*a*, *b*):

$$d\delta[\text{K}]_s/dt = (M_K - M_e - M_d)/\theta^3 \quad (3)$$

where M_e in $\text{M}/\text{cm}^2 \times \text{sec}$ is the net potassium ion flux from the space to the external solution carried by an electric current flowing across the external barrier, M_d in $\text{M}/\text{cm}^2 \times \text{sec}$ is the net potassium ion flux carried by diffusion across the external barrier, and θ is the phenomenological periaxonal space thickness in cm. M_d can be described by the following relation (Frankenhaeuser & Hodgkin, 1956):

$$M_d = \delta[\text{K}]_s \cdot P_{K_s}, \quad (4)$$

where P_{K_s} is the potassium ion permeability of the external barrier in cm/sec.

As the resistance of the external barrier is in series with the excitable membrane, the net current flow across the barrier is the same as that across the membrane. M_e can be described by the following relation (Adelman & Palti, 1969*b*):

$$M_e = I_M \cdot t_K/F \quad (5)$$

where I_M is the total membrane current in amp/cm² as a function of E_M and time, and t_K is the transport number for potassium in the space given by:

$$t_K = [\text{K}]_s/\Sigma([\text{cations}]_0 + [\text{anions}]_0). \quad (6)$$

For TTX-ASW as the external solution, $I_M \simeq I_K$ and we can substitute the following equation for Eq. (5):

$$M_e = I_K \cdot t_K/F. \quad (5a)$$

From the foregoing we obtain:

$$\delta[\text{K}]_s = \left\{ \frac{1}{F} \int_0^{t_1} (I_K) dt - \frac{t_K}{F} \int_0^{t_1} (I_K) dt - P_{K_s} \int_0^{t_1} (\delta[\text{K}]_s) dt \right\} / \theta. \quad (7)$$

From the values of E_K such as those shown in Fig. 3, values of the periaxonal potassium ion concentration¹ $[\text{K}]_s$ were calculated for each t_1 from the Nernst relation as follows:

$$[\text{K}]_s = [\text{K}]_i \exp(E_K F/RT) \quad (8)$$

where $[K]_i$ is the internal potassium ion concentration ², R is the gas constant and T is the absolute temperature. For reasons given in the previous section, a Nernst relation was deemed adequate for describing the potassium current

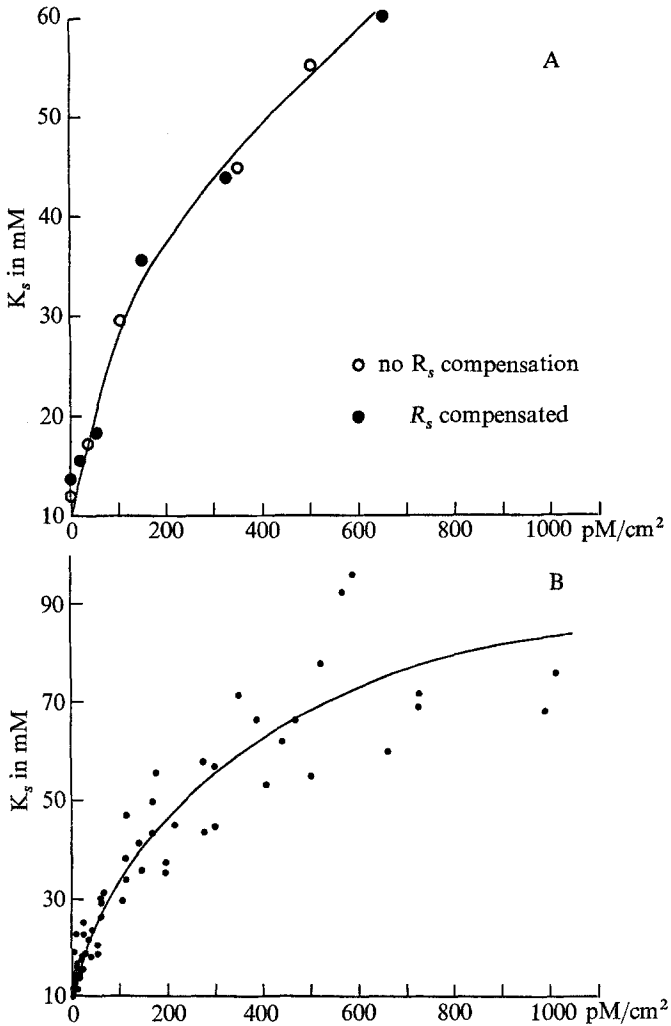


Fig. 6. Concentration of potassium ions in the periaxonal space, K_s (ordinate) plotted against the potassium ion efflux $M_K(t_1)$ (abscissa) in voltage-clamped squid axons bathed in TTX-ASW. *A*: data from axon 4. Values of R_s compensation given in Table 2. *B*: data from axons 1 through 7. Lines in *A* and *B* are curve fits of Eq. (7) to the data points.

See text

² Strictly, activities should be used. However, the error introduced by using concentrations is small if one assumes that the internal and external activity coefficients are about equal (*cf.* Hinke, 1961).

reversal potential. $[K]_i$ was determined from the value of E_K at rest as based on an extrapolation of the early exponential portion (for t_1 values < 5 msec) of E_K vs. t_1 curves to t_0 . In the calculation of $[K]_s$ as a function of t_1 , we have assumed that $[K]_i$ does not vary significantly with t_1 . A 40-msec duration potassium current obtained upon stepping E_M to zero mV, can result in as much as 1,000 pM/cm² of K⁺ ions being moved from inside to outside the axon. This efflux would reduce the internal [K] of a 500- μ diameter axon by only 0.08 mM if there are no diffusion barriers in the interior of the axon.

In Fig. 6A, values of $[K]_s$ calculated from the data in Fig. 3A by means of Eq. (8) are plotted against values of $M_K(t_1)$ shown in Fig. 3B. It is apparent that potassium ion accumulation is a continuous function of $M_K(t_1)$ proceeding smoothly throughout the development of the potassium current. Fig. 6B plots $[K]_s$ vs. $M_K(t_1)$ values obtained from six axons. Thus, Fig. 6B indicates the range of $[K]_s$ values as a function of $M_K(t_1)$ among a group of *Loligo* axons.

Eq. (7) was used to describe the relation between $[K]_s$ and $M_K(t_1)$. For a given E_1 and a set of t_1 values (usually from 1 msec to 40 msec), the values of θ and P_{K_s} were determined by a least-squares curve fit of Eq. (7) to the data using a PDP-11 digital computer. These results are given in Table 2. An indication of the goodness of fit of Eq. (7) to individual experiments is given in Fig. 6A and 7, where the lines are the best fits to the data points.

Table 2. Values of the thickness of the phenomenological periaxonal space θ and the potassium ion permeability of the outer diffusion barrier P_{K_s}

Axon	Temp. (°C)	R_s^a Compen- sated (Ωcm^2)	K_i (mM)	ASW		10% Hyperosmotic ASW			
				θ (\AA)	P_{K_s} (10^{-4} cm/sec)	θ (\AA)	P_{K_s} (10^{-4} cm/sec)	% Inc. (in θ)	% Inc. (in P_{K_s})
1	4.0	None	232.1	281.8	4.37	850.0	3.97	201.6	-9.15
2	6.0	0.66	306.5	205.4	4.24	587.9	4.87	186.2	14.62
3	4.5	1.40	284.3	372.0	2.81				
4a	6.0	1.00	257.0	427.7	4.45				
4b	6.0	None	257.0	417.6	3.80				
5	4.0	None	321.8	325.5	1.51				
6	5.0	None	223.4	231.5	1.89				
7	4.7	None	338.0	594.3	2.61				
		Means	280.4	357.0	3.21				
			$\pm 107.4^b$	$\pm 125.7^b$	$\pm 1.17^b$				

^a Based on current clamp estimate of R_s .

^b Standard deviation.

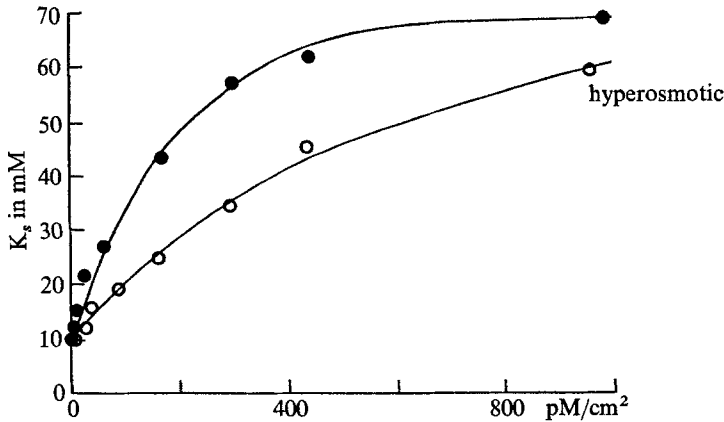


Fig. 7. Concentration of potassium ions in the periaxonal space K_s (ordinate) plotted against the potassium ion efflux $M_K(t_1)$ (abscissa) in a voltage-clamped squid axon bathed in TTX-ASW (filled circles) and in 10% hyperosmotic TTX-ASW (open circles). Lines are least-squares curve fits of Eq. (7) to the data points. Axon 1, uncompensated for R_s .

The line fitting the combined data in Fig. 6B was calculated from Eq. (7) using the mean values of θ and P_{K_s} given in Table 2.

In the use of Eq. (7), water movement which might result from $[K]_s$ changes, is ignored. However, W. K. Chandler (*personal communication*) concluded from his work, that such water movement is very slow and lags behind the ionic changes. In view of the ease of fitting Eq. (7) to the experimental results, it seems justified to assume that any modification of the $[K]_s$ changes by water movement is negligible.

Comparison between Outer Barrier Permeability and the Resistance in Series with the Excitable Membrane

The resistance in series with the membrane R_s can be calculated from the following relation (Frankenhaeuser & Hodgkin, 1956):

$$R_s = (\rho \cdot D) / P'_{K_s}, \quad (9)$$

where D is the diffusion coefficient of 0.5 M KCl at 4.5 °C taken as 1.72×10^{-5} cm²/sec, ρ is the specific resistance of seawater taken as 25 Ω cm, and P'_{K_s} is the permeability of the outer barrier in cm/sec as determined from least-squares curve fits of the relation,

$$P'_{K_s} = \frac{(1/F) \int_0^{t_1} (I_K) dt - \theta' (\delta[K]_s)}{\int_0^{t_1} (\delta[K]_s) dt} \quad (10)$$

Table 3. Values of the thickness of the Frankenhaeuser and Hodgkin space θ' and the potassium ion permeability of the diffusion barrier in series with the Frankenhaeuser and Hodgkin space P'_{K_s}

Axon	θ' (Å)	P'_{K_s} (10^{-4} cm/sec)	R_s (Ωcm^2)
1	290.1	4.73	0.91
2	206.4	4.59	0.94
3	378.8	3.41	1.26
4a	435.8	4.89	0.87
4b	420.7	4.14	1.03
5	607.0	2.99	1.44
6	238.9	2.04	2.10
7	338.1	1.77	2.42
Means	364.5	3.57	1.37
	$\pm 127.5^a$	$\pm 1.22^a$	$\pm 0.67^a$

^a Standard deviation.

to the $M_K(t_1)$ and $[K]_s$ data. This relation which is identical to the form used by Frankenhaeuser and Hodgkin (1956, hypothesis 1) lumps, into one term, all effluxes from the periaxonal space flowing across the outer barrier. P'_{K_s} may then be used to calculate the electrical resistance of the outer barrier by means of Eq. (9). The use of Eq. (9) assumes that R_s is made up mainly of the resistance of the solution in the spaces between Schwann cells and collagen fibers. Values of θ' , the equivalent periaxonal space thickness, P'_{K_s} and R_s are given in Table 3. The mean value of R_s based on eight measurements was $1.37 \Omega \text{ cm}^2$. This value is somewhat larger but comparable to the mean value of $0.77 \Omega \text{ cm}^2$ obtained for the resistance of the Schwann cell-collagen fiber layer as based on current clamp measurements on a larger group of 13 axons (*see* Materials and Methods).

Effect of Hyperosmotic Solution on the Periaxonal Space

When an axon is externally perfused with hyperosmotic seawater, one may expect the axon to decrease in volume. The Schwann cells probably undergo a similar change. This shrinkage should result in an increase of the width of the periaxonal space as well as an increase in the width of the clefts between the Schwann cells. Villegas and Villegas (1960) have shown that Schwann cells swell and the clefts between Schwann cells narrow upon exposing squid giant nerve fibers to hypotonic seawater. Thus, under hyperosmotic conditions, if one accepts the multicompartamental model, it is expected that the periaxonal space thickness θ and possibly the outer

layer potassium permeability P_{K_s} should increase. As a result of the increase in θ , the rate of loading of the space with K^+ during membrane depolarization should decrease. Any increase in P_{K_s} , on the other hand, should result in a decrease in the steady-state value of $[K]_s$ (Adelman & Palti, 1969*b*).

Fig. 7 illustrates the relation between $[K]_s$ and $M_K(t_1)$ obtained for external perfusion of a typical axon with TTX ASW and with 10% hyperosmotic TTX ASW. Note that the rate of change of $[K]_s$ as a function of $M_K(t_1)$ in hyperosmotic ASW is significantly different than in ASW. The least-squares fits (lines) indicate that $\theta = 281.8 \text{ \AA}$ in TTX-ASW and $\theta = 850.0 \text{ \AA}$ in 10% hyperosmotic TTX-ASW. Table 2 lists results obtained on two axons which indicate that 10% hyperosmotic TTX-ASW increases θ by about 200% without significantly changing the values of P_{K_s} .

The Potassium Conductance

The standard method for determining g_K from $I_K/(E-E_K)$ values where E_K is constant (Hodgkin & Huxley, 1952*a*, p. 489) results in different potassium conductance parameter values than those obtained when g_K is derived using driving forces corrected for the changes in E_K . Inasmuch as we have shown that instantaneous I_K vs. E_M relations are quite linear, g_K can be determined from the instantaneous change in I_K upon stepping E_M from one value to another. Under these conditions $\Delta I_K = g_K \cdot \Delta E_K$, the E_K effect cancelling out. One can also use data such as that shown in Figs. 1 and 2 to derive both $g_K(E_M, t)$ and $E_K(E_M, t)$. When either of these methods is used to determine the voltage and time dependency of g_K , new functions describing the voltage dependency of the rate constants for the n process (Hodgkin & Huxley, 1952*b*), α_n and β_n , are obtained.

Fig. 8*A* plots the values of the instantaneous potassium conductance, g_K , against time t_1 , for a set of E_1 values. It is seen that g_K values increase sigmoidally with time for each voltage. Hodgkin and Huxley (1952*b*) derived g_K from a set of I_K vs. time curves by dividing I_K by $(E-E_K)$, E_K being constant. The same set of I_K curves giving rise to the g_K relations shown in Fig. 8*A* were treated in this manner and the results are shown in Fig. 8*B*.

Best fit theoretical curves are drawn through the points in Fig. 8*A* and *B*. These curves are MLAB³ least-squares curve fits (Knott & Reece, 1972; Knott & Shrager, 1972) to the data of the following relation (Hodgkin

³ MLAB (for modeling laboratory) is a large interpretive interactive program which runs on a PDP-10 digital computer time sharing system. It consists of 27 distinct commands which allows the user to define models, specify data, curve-fit, and solve differential equations.

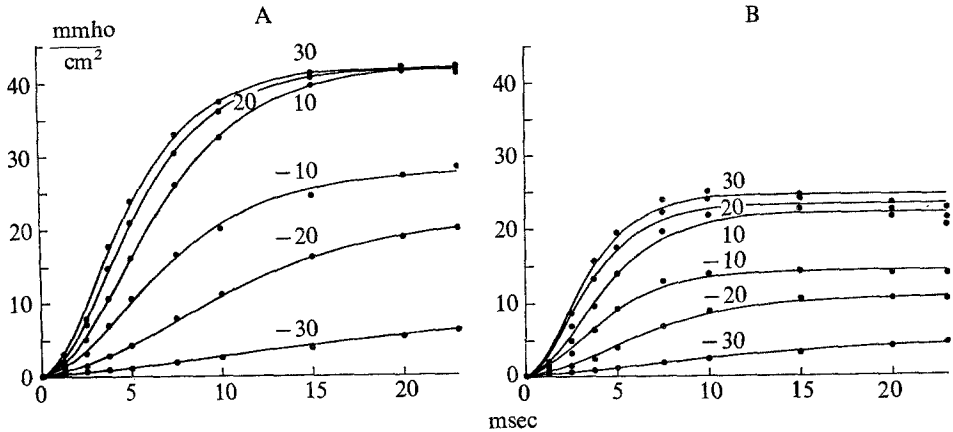


Fig. 8. Development of the potassium conductance g_K (ordinate) as a function of time (abscissa) at the different membrane potentials indicated adjacent to each curve. All data points were derived from delayed membrane currents, corrected for leakage, obtained upon voltage clamping axon 3 in TTX ASW at 4.5 ± 0.1 °C. The curves drawn through the points are least-squares curve fits of Eq. (11) to the data points. In *A*, the points were determined using the relation: $g'_K = I_K / (E - E'_K)$, where E'_K was a variable function of $M_K(t_1)$. The curve fit was obtained for $g_{K0} = 0.2$ mmho/cm² and $\bar{g}_K = 41.77$ mmho/cm². In *B*, the points were determined using the chord conductance relations: $g_K = I_K / (E - E_K)$, where E_K was constant and equal to -80 mV. The curve fit was obtained for $g_{K0} = 0.2$ mmho/cm² and $\bar{g}_K^1 = 24.42$ mmho/cm²

& Huxley, 1952*b*):

$$g_K = \{(g_{K\infty})^{\frac{1}{2}} - [(g_{K\infty})^{\frac{1}{2}} - (g_{K0})^{\frac{1}{2}}] \exp(-t/\tau_n)\}^2 \quad (11)$$

where g_{K0} and $g_{K\infty}$ are the initial and steady-state values of the potassium conductance for a given E_M , and τ_n is the time constant of the n process.

In Fig. 8*B*, steady-state g_K values are less than in Fig. 8*A*. Since the constant E_K method for deriving g_K is not corrected for the E_K shift, these g_K values are only comparable to the instantaneous g_K values at very short depolarizations. Generally, calculating g_K by dividing I_K with $(E - E_K)$, where E_K is held constant, results in smaller values in Fig. 8*B* than the values shown in Fig. 8*A*.

The Voltage-Dependent Rate Constants, α_n and β_n

Inasmuch as any $g_K(t)$ curve for a given E_M rises slower in Fig. 8*A* than the comparable curve in Fig. 8*B*, the Hodgkin-Huxley rate constants for the n process, α_n and β_n must be represented by quantitatively different empirical relations than those given by Hodgkin and Huxley (1952*b*). According to the Hodgkin and Huxley (1952*b*) formalism

$$\alpha_n = n_\infty / \tau_n, \quad (12)$$

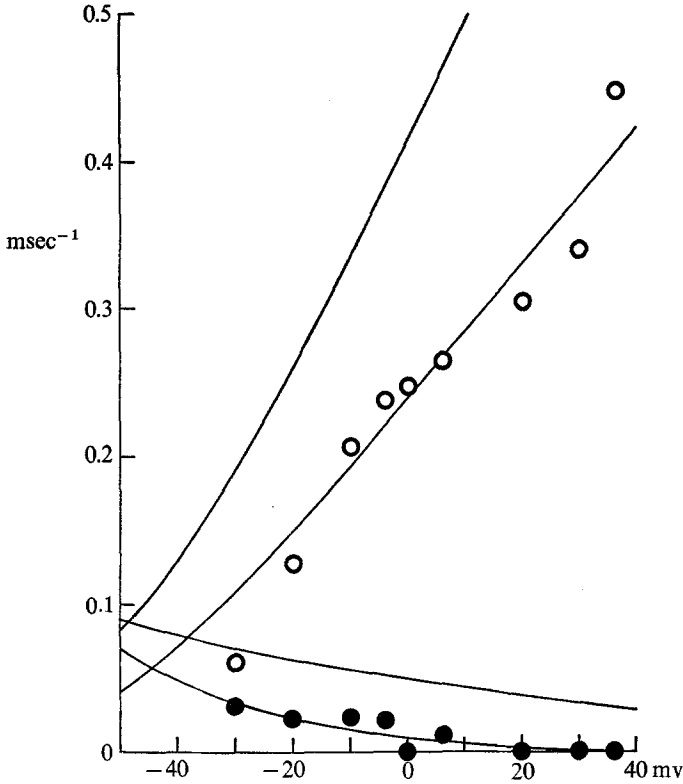


Fig. 9. Values of the rate constants (ordinate) of the rise α_n (open circles) and fall β_n (filled circles) of the potassium conductance at 4.5 °C plotted against membrane potential (abscissa). Values of α_n and β_n were determined by means of Eqs. (11) through (14) from τ_n and n_∞ values obtained from MLAB least-squares curve fits to the data points in Fig. 8A. The curve drawn through the open circles is drawn according to Eq. (19) and the curve drawn through the filled circles is drawn according to Eq. (20). The line drawn somewhat above the open circles is drawn according to Eq. (15) and the line above the closed circles is drawn according to Eq. (16)

and

$$\beta_n = (1 - n_\infty) / \tau_n \quad (13)$$

As

$$n_\infty = (g_{K\infty} / \bar{g}_K)^{\frac{1}{2}} \quad (14)$$

and the MLAB curve fits to the data points in Fig. 8A give the best values of $g_{K\infty}(E_M)$, \bar{g}_K and $\tau_n(E_M)$, a new set of $\alpha_n(E_M)$ and $\beta_n(E_M)$ values can be readily obtained. Fig. 9 plots these values against membrane potential E_M . The lines drawn through the points are the MLAB best fit empirical relations. Hodgkin and Huxley fit their α_n and β_n values with the following relations:

$$\alpha_n = 0.01(-E - 50) / (\exp[(-E - 50)/10] - 1), \quad (15)$$

and

$$\beta_n = 0.125 \exp [(-E - 60)/80]. \quad (16)$$

The MLAB program was used to fit the following relations

$$\alpha_n = A [B - (E + 60)] / \left(\exp \left[\frac{B - (E + 60)}{B} \right] - 1 \right) \quad (17)$$

and

$$\beta_n = C \cdot \exp [(-E - 60)/D] \quad (18)$$

to the data points in Fig. 9 so as to obtain best values for A , B , C , and D . The lines drawn through the points in Fig. 9 are the MLAB best fits to the points. The equations of these lines are:

$$\alpha_n = 0.0046 [7.93 - (E + 60)] / \left(\exp \left[\frac{7.93 - (E + 60)}{7.93} \right] - 1 \right), \quad (19)$$

and

$$\beta_n = 0.1 \cdot \exp [(-E - 60)/26.72]. \quad (20)$$

The other two lines are plots of Eqs. 15 and 16 corrected to 4.5 °C using a Q_{10} of 3.

Discussion

The results presented here confirm the findings of Frankenhaeuser and Hodgkin (1956) with respect to potassium accumulation in the periaxonal space. In addition, evidence is given indicating that this effect is a continuous function throughout the course of development of a membrane potassium current. Frankenhaeuser and Hodgkin found that the potassium accumulation external to the axolemma in repetitively firing axons fitted a multi-compartmental model better than an unstirred layer type model. The experimental data described in this work agrees well with such a multi-compartmental model. Inasmuch as P'_k values in Table 3 were obtained using an equation identical with that used by Frankenhaeuser and Hodgkin (1956), these values may be compared with the P_{k_s} values obtained by Frankenhaeuser and Hodgkin. Our mean value of 3.57×10^{-4} cm/sec is about an order of magnitude larger than Frankenhaeuser and Hodgkin's value of 6.0×10^{-5} cm/sec. One explanation for this difference is that the outer barrier in *Loligo pealei* axons is more permeable to potassium ions than the outer barrier in *Loligo forbesi* axons.

While our results suggest that the multicompartmental approach, rather than an "unstirred layer" approach (Frankenhaeuser & Hodgkin, 1956, hypothesis 2), provides an adequate description of the axon behavior, the most important evidence in favor of the multicompartmental model arises from the behavior of axons in hyperosmotic ASW. When exposed to mildly hyperosmotic ASW, axons shrink. In 10% hyperosmotic ASW, the measured

decrease in axon diameter was 5 to 10%. Since, under these conditions the Schwann layer cells are also expected to lose some of their volume, the space between the axolemma and Schwann layer is expected to widen, and this should result in a slower rate of loading of the space and indeed $\delta[K]_s$ was slower as a function of membrane potassium ion efflux under these conditions (*see* Fig. 7).

The intercellular pathways between Schwann cells, through which water and ions are generally believed to flow (Villegas *et al.*, 1962), should widen in hyperosmotic ASW since under such conditions the Schwann cells presumably shrink. As the length of these pathways is many orders of magnitude larger than their diameter (Villegas & Villegas, 1960), any increase in the cross-section of the pathways should not result in a significant increase in the outer layer potassium permeability P_{K_s} (Villegas *et al.*, 1962, p. 253). The experimental results in Table 2 are consistent with this hypothesis. We may thus conclude that, since the rate of K accumulation appears to vary with the periaxonal space width, there is some justification in using the multicompartmental model to describe the potassium accumulation phenomenon.

In this regard, it is interesting to compare the squid axon studies with studies conducted on other neural tissues. Kuffler, Nicholls and Orkand (1966) have shown that the membrane potential of amphibian glial cells varies with the extracellular [K]. As glial cells depolarize whenever adjacent neurons fire repetitively, Orkand *et al.* (1966) claimed that neuronal repetitive activity results in an accumulation of K in the 150 Å-thick perineuronal space found between the active neurons and the adjacent glial cells.

Baylor and Nicholls (1969*a, b*) studied repetitive firing in leech neurons and were able to show that during a train of impulses, the undershoot phase of the action potential becomes progressively less negative as the duration of the train increases. Upon considering that the undershoot potential approximates a potassium ion reversal potential (Frankenhaeuser & Hodgkin, 1956), they were able to interpret these results by assuming that potassium ions accumulate in the 150 Å-thick perineuronal space found between the neurons and the glial cells. In addition, Baylor and Nicholls (1969*a*) were able to eliminate the changes in action potential undershoot associated with repetitive activity by physically removing the glial cells around the neurons. This experiment suggests that the assumed potassium accumulation in perineuronal spaces is dependent on an intact external barrier (the glial cells) to the diffusion of potassium ions away from the neuron surface. This finding further justifies the use of the multicompartmental model in describing the potassium ion accumulation phenomenon.

The evidence presented in this paper indicates that potassium ion accumulation in the periaxonal space attenuates the potassium driving force and thus must have a negative feedback effect upon potassium currents. This effect is readily illustrated by the "droop" in outward potassium currents persisting longer than 10 msec (Fig. 1).

The results shown in Figs. 8 and 9 indicate that this feedback effect should be considered whenever deriving ionic conductances or conductance parameter values from membrane potassium currents. Not only are \bar{g}_K and g_{K_∞} values larger when this is considered, but the values of the Hodgkin and Huxley rate constants for the n process are smaller, indicating a slower conductance turn-on with voltage than expected.

Frankenhaeuser and Hodgkin (1956) state that, "One limitation of the theory put forward by Hodgkin and Huxley (1952*b*) on the basis of voltage clamp records is that the equations do not predict a negative after-potential. It is now evident that this limitation arose because the analysis took no account of the polarization effect observed with large outward currents". In a subsequent paper it will be shown that with \bar{g}_K , α_n and β_n values such as are shown in Figs. 8 and 9 and with appropriate corrections made for K_s accumulation, this limitation can be partially overcome (Adelman, FitzHugh & Palti, *in preparation*).

The significance of potassium accumulation reaches beyond the above-described effects in axons. Sjodin (1971) has recently reviewed the evidence for the transport of sodium and potassium ions across the axolemma and other living membranes as a function of the external potassium ion concentration. In the central nervous system natural repetitive activity of axons and neurons must result in K^+ accumulation. The resulting K_s changes will affect the firing rates, integrative functions, transmitter release, etc., in these systems (Baylor & Nicholls, 1969*a*). For example, during hyperpolarization which follows a train of impulses the neuron membrane is hypersensitive to external potassium (Baylor & Nicholls, 1969*b*; Jansen & Nicholls, 1973), and the K_s effect may be considerably amplified under a variety of conditions.

In addition, some widespread CNS phenomena such as spreading cortical depression (Grafstein, 1956, 1963) and epileptiform cortical discharges (Fertziger & Ranck, 1970) have been explained on the basis of changes in $[K]_s$. The role of $[K]_s$ in modifying the activity of both peripheral and central nervous systems has been reviewed recently by Adelman and Palti (1972*a*).

The authors thank Joseph Patlak for expert technical assistance, John M. Shaw and Richard FitzHugh for assistance with the least-squares curve fitting programs, and Harold Lecar for reading and criticizing the manuscript.

References

- Adelman, W. J., Jr., Palti, Y. 1969*a*. The influence of external potassium on the inactivation of sodium currents in the giant axon of the squid, *Loligo pealei*. *J. Gen. Physiol.* **53**:685
- Adelman, W. J., Jr., Palti, Y. 1969*b*. The effects of external potassium and long duration voltage conditioning on the amplitude of sodium currents in the giant axon of the squid, *Loligo pealei*. *J. Gen. Physiol.* **54**:589
- Adelman, W. J., Jr., Palti, Y. 1972*a*. The role of periaxonal and perineuronal spaces in modifying ionic flow across neural membranes. *In*: Current Topics in Membranes and Transport. F. Bronner and A. Kleinzeller, editors. Vol. 3, p. 199. Academic Press Inc., New York
- Adelman, W. J., Jr., Palti, Y. 1972*b*. Some relations between external cations and the inactivation of the initial transient conductance in the squid axon. *In*: Perspectives in Membrane Biophysics. D. P. Agin, editor. p. 101. Gordon and Breach Science Publishers, Inc., London
- Baker, P. F., Hodgkin, A. L., Shaw, T. I. 1962. Replacement of the axoplasm of giant nerve fibres with artificial solutions. *J. Physiol.* **164**:330
- Barry, P. H., Hope, A. B. 1969*a*. Electroosmosis in membranes: Effects of unstirred layers and transport numbers. I. Theory. *Biophys. J.* **9**:700
- Barry, P. H., Hope, A. B. 1969*b*. Electroosmosis in membranes: Effects of unstirred layers and transport numbers. II. Experimental. *Biophys. J.* **9**:729
- Baylor, D. A., Nicholls, J. G. 1969*a*. Changes in extracellular potassium concentration produced by neuronal activity in the central nervous system of the leech. *J. Physiol.* **203**:555
- Baylor, D. A., Nicholls, J. G. 1969*b*. After-effects of nerve impulses on signalling in the central nervous system of the leech. *J. Physiol.* **203**:571
- Carpenter, D. O., Hovey, M. M., Bak, A. F. 1971. Intracellular conductance of aplysia neurons and squid axon as determined by a new technique. *Int. J. Neurosci.* **2**:35
- Carpenter, D. O., Hovey, M. M., Bak, A. F. 1972. Intracellular conductivity measurements in giant neurons, axons and muscle fibers. *Soc. for Neuroscience, Second Annual Meeting, (Abstracts)*, Houston, Texas, October 8–11, 1972, p. 18
- Cole, K. S., Moore, J. W. 1960. Ionic current measurements in the squid axon membrane. *J. Gen. Physiol.* **44**:123
- Cuervo, L. A., Adelman, W. J., Jr. 1970. Equilibrium and kinetic properties of the interaction between tetrodotoxin and the excitable membrane of the squid giant axon. *J. Gen. Physiol.* **55**:309
- Fertziger, A. P., Ranck, J. B., Jr. 1970. Potassium accumulation in interstitial space during epileptiform seizures. *Exp. Neurol.* **26**:571
- Frankenhaeuser, B., Hodgkin, A. L. 1956. The after-effects of impulses in the giant nerve fibres of *Loligo*. *J. Physiol.* **131**:341
- Geren, B. B., Schmitt, F. O. 1953. The structure of the nerve sheath in relation to lipid and lipid-protein layers. *J. Appl. Physiol.* **24**:1421
- Geren, B. B., Schmitt, F. O. 1954. The structure of the Schwann cell and its relation to the axon in certain invertebrate nerve fibers. *Proc. Nat. Acad. Sci.* **40**:863
- Grafstein, B. 1956. Mechanism of spreading cortical depression. *J. Neurophysiol.* **19**:154
- Grafstein, B. 1963. Neuronal release of potassium during spreading depression. *In*: Brain Function. M. A. B. Brazier, editor. p. 87. Elsevier Press, New York
- Hinke, J. A. M. 1961. The measurement of sodium and potassium activities in the squid axon by means of cation-selective glass microelectrodes. *J. Physiol.* **156**:314
- Hodgkin, A. L., Huxley, A. F. 1952*a*. The components of membrane conductance in the giant axon of *Loligo*. *J. Physiol.* **116**:473

- Hodgkin, A. L., Huxley, A. F. 1952*b*. A quantitative description of membrane current and its application to conduction and excitation in nerve. *J. Physiol.* **117**:500
- Hodgkin, A. L., Huxley, A. F., Katz, B. 1952. Measurement of current-voltage relations in the membrane of the giant axon of *Loligo*. *J. Physiol.* **116**:424
- Jansen, J. K. S., Nicholls, J. G. 1973. Conductance changes, an electrogenic pump and the hyperpolarization of leech neurons following impulses. *J. Physiol.* **229**:635
- Keynes, R. D. 1951. The ionic movements during nervous activity. *J. Physiol.* **114**:119
- Keynes, R. D., Lewis, P. R. 1951. The sodium and potassium content of cephaloped nerve fibres. *J. Physiol.* **114**:151
- Knott, G. D., Reece, D. K. 1972. MLAB: A civilized curve-fitting system. *Proc. ONLINE '72 Int. Conf.*, Brunel University, England
- Knott, G. D., Shrager, R. I. 1972. On-line modeling by curve-fitting. *Proc. SIGGRAPH Computers in Med. Symp., ACM, SIGGRAPH Notices*
- Kuffler, S. W., Nicholls, J. G., Orkand, R. K. 1966. Physiological properties of glial cells in the central nervous system of amphibia. *J. Neurophysiol.* **29**:768
- Metuzals, J., Izzard, C. S. 1969. Spatial patterns of threadlike elements in the axoplasm of the giant nerve fiber of the squid (*Loligo pealei* l.) as disclosed by differential interference microscopy and by electron microscopy. *J. Cell Biol.* **43**:456
- Moore, J. S., Cole, K. S. 1963. Voltage clamp techniques. *In: Physical Techniques in Biological Research*. W. L. Nastuk, editor. Vol. 6, p. 263. Academic Press Inc., New York
- Orkand, R. K., Nicholls, J. G., Kuffler, S. W. 1966. Effect of nerve impulses on the membrane potential of glial cells in the central nervous systems of amphibia. *J. Neurophysiol.* **29**:788
- Shanes, A. M. 1954. Effect of temperature on potassium liberation during nerve activity. *Amer. J. Physiol.* **177**:377
- Sjodin, R. A. 1971. Ion transport across excitable cell membranes. *In: Biophysics and Physiology of Excitable Membranes*. W. J. Adelman, Jr., editor. Ch. 3, p. 96. Van Nostrand Reinhold Co., New York
- Villegas, G. M. 1969. Electron microscopic study of the giant nerve fiber of the giant squid *Dosidicus gigas*. *J. Ultrastruct. Res.* **26**:501
- Villegas, R., Caputo, C., Villegas, L. 1962. Diffusion barriers in the squid nerve fiber. The axolemma and the Schwann layer. *J. Gen. Physiol.* **46**:245
- Villegas, R., Villegas, G. M. 1960. Characterization of the membranes in the giant nerve fiber of the squid. *J. Gen. Physiol.* **43**:(Suppl.) 73